SEARCH Atmospheric Element 1: Retrospective Analysis of Arctic Clouds and Radiation from Surface and Satellite Measurements

FINAL REPORT

to the
National Oceanic and Atmospheric Administration (NOAA)
for funding under the SEARCH program

Reporting period:
May 1, 2003 through September 12, 2006

Project PIs:
Jeffrey R. Key
Office of Research and Applications, NOAA/NESDIS
Madison, Wisconsin

Taneil Uttal
NOAA/PSD, Boulder, Colorado

Robert Stone
Cooperative Institute for Research in the Environmental Sciences
University of Colorado, and NOAA/GMD, Boulder, Colorado

Collaborators:
Xuanji Wang
Cooperative Institute for Meteorological Satellite Studies (CIMSS)
University of Wisconsin, Madison, Wisconsin

Shelby Frisch
Cooperative Institute for Research of the Atmosphere
Colorado State University and NOAA/PSD, Boulder, Colorado

Matthew Shupe
Cooperative Institute for Research in the Environmental Sciences
University of Colorado, and NOAA/PSD, Boulder, Colorado

September 21, 2006

Table of Contents

Purpose

This report serves as summary of work done on Element 1 of the NOAA SEARCH project at the Cooperative Institute for Meteorological Satellite Studies (CIMSS), University of Wisconsin-Madison (UW), the NOAA Physical Science Division, Boulder, CO, CIRES/University of Colorado-Boulder, and CIRA/Colorado State University-Fort Collins.

Objectives

The objective of this element was to evaluate the degree to which historical and ongoing measurements can be used to answer SEARCH science questions and to aid in the evaluation of optimum locations for an expansion of the Arctic observing network (Element 3). The task was to perform a retrospective analysis of coincident surface measurements and satellite-derived quantities, comparing one to the other, and assessing the spatial and temporal variability in each parameter.

Our focus was on clouds and radiation but attention was also given to surface properties, especially pertaining to recent trends in Arctic snow cover, surface temperatures and sea ice that can induce a temperature-albedo feedback. Appropriate improvements in algorithms were made, but the emphasis was on data analysis, not algorithm development. This work also supported the SEARCH Reanalysis Project (Element 7) that aims to exploit a variety of polar data sets and reanalysis products used in model studies, and to provide preliminary comparison of trends at the proposed Intensive Observatory sites (Element 1) at Barrow, Tiksi, Alert and Eureka.

The research summarized in this report addressed the following SEARCH science questions:

- How can we characterize the composition, scales, and persistence of the recent complex of dramatic environmental changes in the Arctic system?
- Are the changes consistent with natural variability, or do the climate changes involve an anthropogenic origin? How unusual are the changes in the context of instrumental and proxy records as well as model-based studies?
- What are the critical interactions among ocean, ice, land, and atmosphere that can be related to identifiable climate patterns such as the Arctic Oscillation?
- Do albedo feedbacks from snow and sea ice extend the duration of melt season anomalies?
- How are global climate and Arctic variability coupled?
- How does the current warming trend affect sea ice and can it initiate ice-albedo feedbacks?

It should be noted that when this work was initiated the Arctic Oscillation was considered to be major control on dramatic changes that were being observed in the Arctic (termed “Unaami”). During the period 2000-2005 when much of this work was accomplished, the relationship between changing variables and the Arctic Oscillation has appeared to have significantly weakened. This has resulted in some adjustment of the SEARCH science questions that were addressed in this report.

Personnel

The lead scientist for this project at NOAA/NESDIS and UW/CIMSS is Jeff Key. Xuanji Wang, a CIMSS postdoc, performed most of the satellite data retrievals. Yinghui Liu, a PhD student, performed additional data analyses. Their research involved the use of satellite data to estimate surface, cloud, and radiation properties over the Arctic, both on short and long time scales. Taneil Uttal, NOAA/PSD, and Robert Stone, CIRES/CU and NOAA/GMD, are Co-Principal Investigators on this element of the

NOAA SEARCH program. Additional analyses were performed by Matthew Shupe of CIRES/CU and Shelby Frisch of CIRA/CSU. Their research involved surface-based cloud radar, radiation, and meteorological measurements, and comparison between surface and satellite data sets.

Summary of Accomplishments

Our accomplishments for Element 1 include:

1. Satellite retrieval techniques for use with the AVHRR Polar Pathfinder (APP) dataset were refined and validated with data from SHEBA and from Barrow, Alaska.
2. Surface, cloud, and radiation characteristics for 23 years of APP data, covering the period 1982-2004, have been estimated, and a data product has been made available to the public. The new product is called the extended AVHRR Polar Pathfinder, or APP-x.

    - An analysis of trends shows that the Arctic has been cooling at the surface during the winter, particularly over the ocean, but warming at other times of the year, particularly over land. The surface albedo has decreased, especially during the autumn months. Cloud amount has been decreasing during the winter but increasing in spring and summer. During summer, fall, and winter, cloud forcing has tended toward increased cooling (or decreased warming). This implies that if Arctic cloud cover had not been changing the way it has over the past two decades, surface temperatures would probably have risen at an even greater rate than what has been observed.
    - Decreases in sea ice extent and albedo that result from surface warming modulate the increasing cloud cooling effect, resulting in little or no change in the radiation budget.
    - Changes in summer albedo over Alaska correlate with a lengthening of the snow-free season that has increased atmospheric heating locally by 3 W/m-2/decade. Current trends in shrub and tree expansion could further amplify this by 2-7 times. (Done in collaboration with T. Chapin, University of Alaska)

3. The APP-x product was used in combination with horizontal heat and moisture advection derived from the TIROS Operational Vertical Sounder (TOVS) Path-P product, and with clear sky temperature inversion data derived from the High Resolution Infrared Radiation Sounder (HIRS, part of TOVS). The goal was to examine the relationship between trends in cloud properties, temperature inversion characteristics, advection, and surface radiation. This work was done with J. Francis, Rutgers University, and Y. Liu, CIMSS (both funded separately).

    - The decreasing trend in winter surface temperature over the central Arctic cannot be explained solely by large-scale atmospheric circulation changes. There is a strong coupling between changes in surface temperature and changes in inversion strength, but that trends in some areas may be a result of advection aloft rather than warming/cooling at the surface.
    - Other researchers have reported that the loss of Arctic perennial ice cover is almost 10% per decade. We found that the relative roles of advection and radiation in this process vary by region.

4. Trajectory analyses have been performed to produce Arctic station climatologies by season.
5. The snowmelt record of Barrow, Alaska (BRW) was re-examined to substantiate a previously reported trend towards an earlier date of spring melt over Northern Alaska, 1941-2003.

    - Analyses corroborated earlier findings that diminished snowfall during winter and warmer spring temperatures are the cause. The onset and duration of the melt season over the western

  Arctic Ocean was found to correlate with the BRW snowmelt record, suggesting that the same dynamical and radiative processes influence sea ice distribution and snow cover on land. Also, early snowmelt over southern land areas tends to accelerate the melt of sea ice due to enhanced warm air advection.
- There appears to be a precedent for the extreme years of early snow melt that occurred from 1990 to about 2003, which gave rise to a significant trend when considering only the recent period. This perspective needs further verification and explanation because it has a bearing on how we interpret recent trends in sea ice concentration, which correlates with snow cycles through dynamic and thermodynamic processes.

6. A retrospective analysis of aerosol optical depth measurements derived from BRW sunphotometer data was performed.

   - The analysis revealed distinctive spectral signatures in Arctic Haze and Asian Dust. These are two aerosol types that can perturb the radiometric structure of the Arctic atmosphere, and possibly influence cloud microphysical properties. Using model and empirical results to quantify the direct forcing on the surface radiation balance at BRW by Asian Dust, it was shown that a modest layer of dust has a cooling effect that exceeds the warming effect of a doubling of CO_2.

7. An 8-year record of cloud microphysics, cloud forcing data and cloud statistics was compiled for the North Slope of Alaska. This data was used to examine the reliability of the surface-based radar data for cloud studies, determine the relative importance of cloud fraction and cloud optical depth on surface cloud forcing, develop spectra techniques for determining cloud phase from radar data, determine the relative occurrence of clouds with liquid water, ice crystals and mixed phase, and study mixed phase cloud properties.

8. Comparisons have been undertaken between surface-derived cloud fraction and optical depth and satellite cloud microphysics for (1) the APP-X data set, (2) the MODIS-based cloud microphysics from the NASA/CERES team, (3) a TOVS data set, and (4) the standard MODIS cloud products, and (5) the PATMOS-X cloud products.

9. Comparisons of multi-decadal APP-x satellite surface temperature data for Barrow, Eureka, Alert and Tiksi with in-situ measurements of surface temperature. These comparisons indicate that:

   - Depending on season, there may be biases in the satellite determined surface temperatures that are a function of cloud fraction.
   - The different regions represented by Barrow, Eureka Alert and Tiksi may have different biases indicating the need for studies in different Arctic regions.
   - The surface data sets may allow for correction of biases in the satellite data sets that can be applied to regions over which there are no surface data sets for comparison.

10. Using the APP-x data, trends in cloud fraction and optical depth were examined for Barrow, Eureka, Alert and Tiksi to assess regional variability at the locations proposed for Intensive Observatories (Element 3).

Details on these accomplishments are given in the following sections.

Retrospective Satellite Analyses

Satellite retrieval techniques for use with the AVHRR Polar Pathfinder (APP) dataset have been refined and validated. Retrieved parameters are surface temperature, surface albedo, cloud properties (fraction, type, particle phase, effective radius, optical depth, temperature, and pressure), and radiative fluxes under all-sky conditions. Data from the SHEBA experiment and two Antarctic meteorological stations have been used for validation.

Twenty-three (23) years of APP data from the National Snow and Ice Data Center (NSIDC) have been acquired and processed. The twice-daily data cover the period 1989-1999 at a spatial resolution of 25 x 25 km^2, subsampled from the original 5 x 5 km^2 data. The area of coverage is shown in Figure 1. Monthly and seasonally averaged products were also created and archived. The extended APP dataset (APP-x) has been made available to the community for a variety of data comparisons and applications.

Figure 2 shows the annual cycle of total cloud amount from the surface observations, the International Satellite Cloud Climatology Project (ISCCP) D2 product, the TOVS Path–P dataset, and the extended AVHRR Polar Pathfinder (APP-x). The data in Figure 2 are averaged over the period 1982-1991. The surface-based climatology does not include clear sky ice crystal precipitation (ICP). ICP occurs in wintertime 20-50% of the time and may be optically thick enough to have a significant radiative effect. Overall, satellite derived products (APP-x) show good agreement with surface-based measurements, e.g., the biases between SHEBA ship measurements and APP-x dataset are 0.2 K in surface temperature, -0.05 (absolute) in surface broadband albedo, 9.8 Wm^{-2} in the downwelling shortwave radiation flux, and 2.1 Wm^{-2} in the downwelling longwave radiation flux.

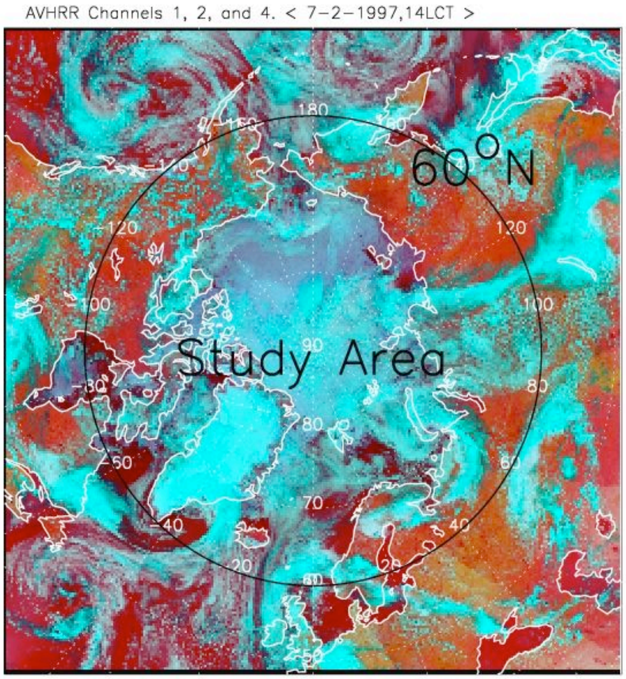

Fig. 1. The spatial coverage of the APP dataset during the period of 1982–2004. The image is a true color three channel (AVHRR channels 1, 2 and 4) composite.

Spatial and temporal characteristics of Arctic surface, cloud properties and radiative fluxes have been investigated. The daily APP-x composite data used here are centered on local solar times of 04:00 and 14:00. The area north of 60°N latitude is of primary interest. The twice-daily results were averaged to obtain monthly, seasonal and yearly mean results. Figure 3 shows the annual cycles of cloud and radiation properties in the Arctic at 14:00. Examples of the spatial distribution of cloud amount and surface skin temperature at 14:00 are given in Figure 4.

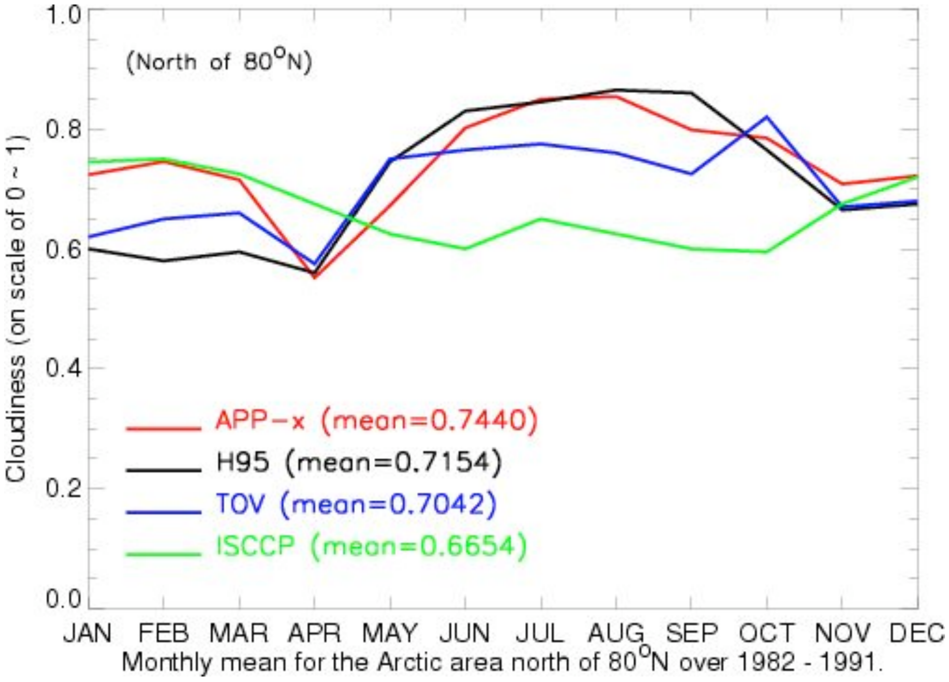

Fig. 2. The annual cycle of cloud amount from surface-based observations (H95) and satellite retrievals (ISCCP-D2, TOVS Path-P, and APP-x).

In general, the Arctic surface temperature varies most over the landmasses, and least over the Arctic Ocean. Greenland is the coldest place in the Arctic all the year round. The Arctic is also one of the cloudiest regions on the earth, with an annual mean cloud cover of about 70%. The visible cloud optical depth is about 5~6 on the annual average. Cloud top pressures are on average in the range 750-600 hPa except over Greenland where the average is approximately 600~450 hPa.

Trends in surface, cloud properties, and radiative fluxes, as well as their uncertainties and statistical significance, were investigated. The ocean area north of 60° latitude has been cooling at the surface during the winter, but the Arctic overall has been warming at other times of the year and on the annual average. The wintertime surface temperature has decreased at the decadal rate of –0.38 degrees, but all other seasons have warming trends; the largest warming occurred in spring at the decadal rate of 0.88 degrees. The wintertime decrease has also been observed in surface measurements and in the TOVS data record (A. Schweiger, pers. comm., 2003). The surface albedo has decreased, particularly during the summer and autumn months. Cloud amount has been decreasing during the winter but increasing in spring (daytime). Changes in cloud amount - increasing spring, summer, and autumn, but decreasing in winter - result in cloud radiative forcing that tends toward increased cooling (or decreased warming). This implies that if seasonal cloud amount had not changed as observed, surface warming would have been even greater.

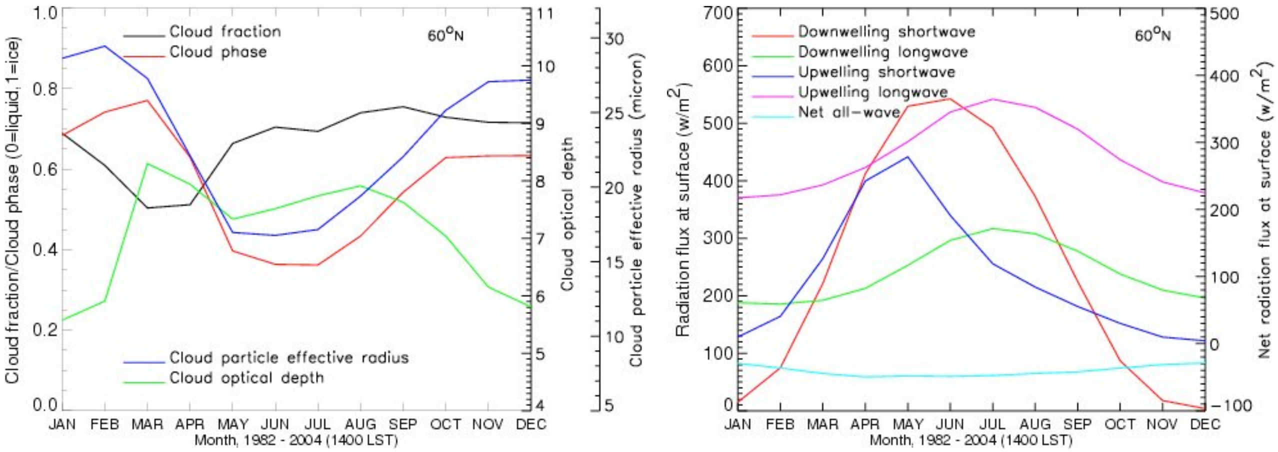

Fig. 3. Annual cycle of cloud fraction, cloud optical depth, cloud particle effective radius and cloud particle phase (left), and surface radiative fluxes (right) from APP-x.

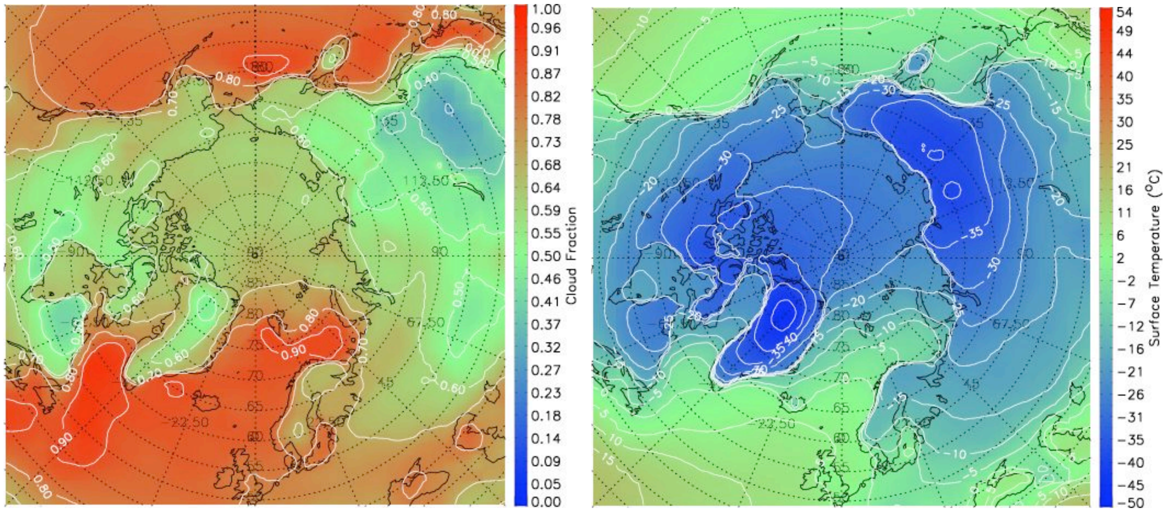

Fig. 4. The spatial distribution of cloud fraction (left) and surface skin temperature (right) at 14:00 local time for the period 1982-2004.

Figure 5 shows the trends of surface temperature, surface broadband albedo, and cloud fraction in winter, spring, summer, autumn, and annually for the area north of 60°N at 14:00 local solar time. Surface temperature has increased for all seasons except for winter, and cloud fraction has increased during the Arctic spring, but decreased for other seasons. An example of the spatial variability in the wintertime surface temperature trend is also shown in Figure 5.

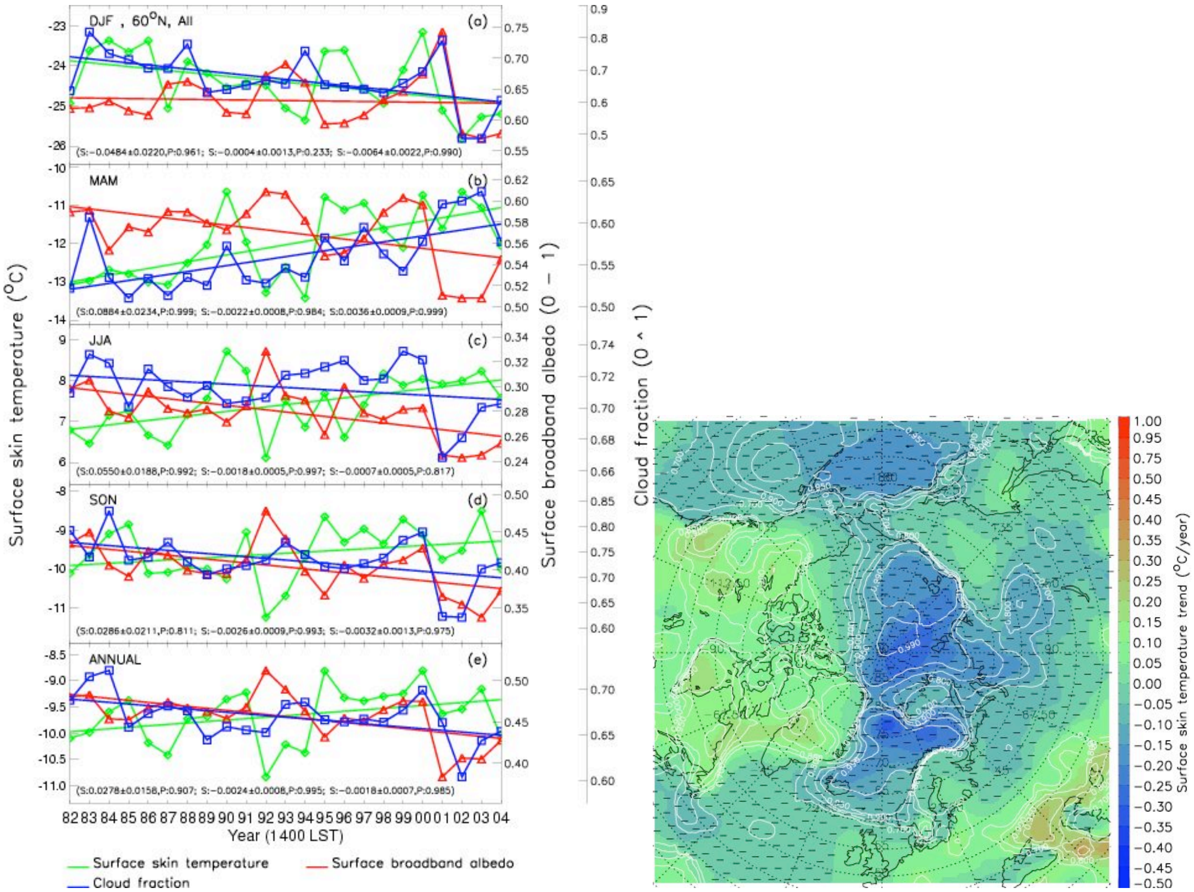

Fig. 5. **Left**: Time series and trends in surface temperature, surface broadband albedo, and cloud fraction in winter (DJF), spring (MAM), summer (JJA), autumn (SON) and annual average (ANN) over the area north of 60°N at 14:00. The numbers in parentheses are the slope of the trend with its uncertainty and F test confidence level, where S stands for slope per year and P for confidence level for that slope. The first group of S and P denotes surface temperature trend (green line); the second group denotes surface broadband albedo trend (red line), and the last group denotes cloud fraction trend (blue line). **Right**: The spatial distribution of the trends in surface temperature over the period of 1982 – 2004 in winter at 14:00. The contours are confidence levels.

Retrospective Analyses of the Western Arctic

Back Trajectory Analysis

A trajectory analysis was performed to produce several Arctic station climatologies by season. An example for Alert, Canada, a site that is currently being enhanced as part of Element 3, is shown in Figure 6. Climatologies for four prospective Siberian sites were also generated (not shown). These are valuable for understanding flow patterns that influence cloud distribution and aerosol concentrations at these locations. At Alert, for instance, the flow at 1500 m is from central Greenland about 20% of the time during all seasons except summer. About 20% of the flow during all seasons is of local origin, northerly during winter/spring but southwesterly in summer and autumn. Long Range flow from Eurasia is common, especially during winter and spring. On this basis Arctic Haze probably is transported to Alert annually.

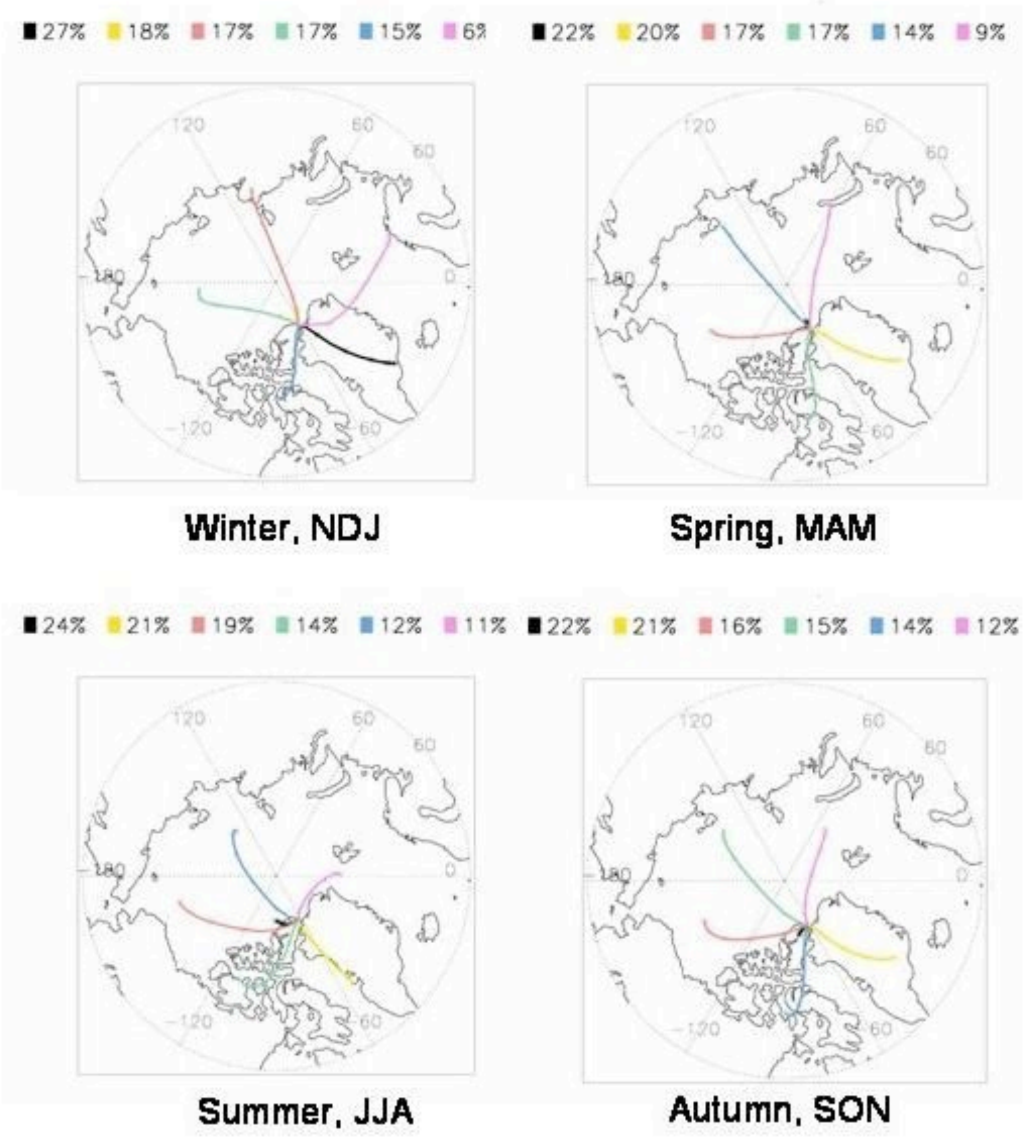

Fig. 6. Back trajectory climatology for Alert, Canada. The frequencies of six principal flow patterns are color coded as labeled. The arrival altitude is 1500 m, and the seasonal means are generated for all years, 1986-2002.

Correlated Trends in Sea Ice Extent and Snow Cover in the Western Arctic

Following a previous study that documented a trend in the date when snow melts (melt date) at Barrow (BRW) in spring, an update was made and examined in the context of the entire western Arctic, including oceanic regions northwest of Barrow (Levinson and Waple, 2004). Although 1999, 2000, and 2001 were years of moderately late snowmelt at BRW, 2002 was the earliest on record. The 2003 melt was again early (Figure 7) further substantiating a trend towards an earlier spring melt in northern Alaska.

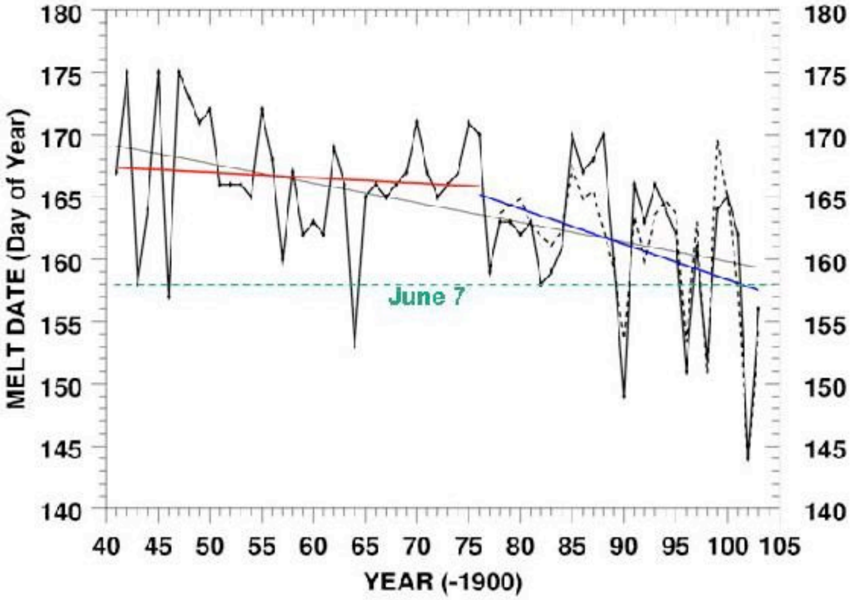

Fig. 7. Time series of snow melt dates constructed for the NOAA/CMDL Barrow Observatory. Three linear regressions are plotted: an overall fit for 1941-2003 (thin black line), one for all years prior to 1977 (red), and a third beginning in 1977 (blue). Results of an empirical model are also shown (dashed). The time series was compiled from direct snow depth observations, proxy estimates using daily temperature records, and beginning in 1986 on the basis of surface radiometric measurements (updated from Stone et al., 2002).

Through 2003, the spring melt at BRW had advanced by about 10 days (+/- 4.8 d, 95% confidence interval) since 1940. Most of the advance occurred after 1976 when a major regime shift occurred in many climatic as well as biological indicators of climate change. Variations in the annual snow cycle of northern Alaska are attributable, in large part, to changes in atmospheric circulation that involve intensification of the Aleutian Low (AL) pressure center in conjunction with fluctuations of the Beaufort Sea Anticyclone (BSA). On this basis, an empirical model was developed to predict melt dates at BRW. Results are shown as a dashed curve in Figure 7. About 80% of the variance in melt dates at BRW can be explained by changes in snowfall during winter, and variations in springtime temperatures and cloudiness.

Using passive microwave data from polar orbiting satellites, the onset of snowmelt on sea ice can be determined. Comparisons of time series of sea ice melt offshore Alaska with the timing of snowmelt across the North Slope of Alaska reveal a region of high correlation near the climatological center of the

BSA. Analyses suggest that variations in the position and intensity of the BSA have far reaching effects on the annual accumulation and subsequent melt of snow and ice over a large region of the western Arctic.

Spring appears to be a critical transition period in the annual cycles of snow and sea ice. During years of early melt onset there tends to be a complete breakdown of the BSA during spring. In the absence of this High, the transport of warm, moist air into the Arctic is unrestricted. The enhanced advection of warm air also adds moisture to the Arctic atmosphere, increasing cloudiness. Increased cloud cover in spring is corroborated by independent analyses of the extended AVHRR Polar Pathfinder satellite data product. Prolonged effects of warm air advection augmented by thermal emissions from clouds (cloud radiative forcing) can modify the microphysical structure of the snow pack. It is thought that this "ripening" may precondition the snow such that the melt is accelerated during May/June when solar insolation reaches its annual peak. The depth of snow on sea ice prior to the onset of melt is also important because significant ice melt cannot occur until the insulating layer of snow melts first. It is suggested that reduced snowfall over the western Arctic Ocean in recent years may account, in part, for the decline in sea ice in that region. The influence of regional circulation on the disposition of snow and ice during the spring/summer transition is illustrated in Figure 8, which compares average environmental conditions for four years of extreme ice retreat (1998, 2002-2004) with a period during which ice retreat was minimal (1985-1988). Mean fields of 850 mb geopotential heights represent synoptic patterns for spring. Geopotential is commonly used as a vertical coordinate when describing large-scale flow patterns, where larger values at a prescribed pressure level indicate higher atmospheric pressure.

Figure 8a illustrates typical climatological conditions during March, April and May in the western Arctic. The BSA and AL are strongly coupled forming a north-south dipole pattern. The BSA effectively blocks Pacific air from flowing into the Arctic. Such a pattern keeps northern regions cold and relatively dry and constrains the circulation of ice within the Beaufort Sea. Climatologically, in late May, the North Slope of Alaska and eastern Siberia remain covered in snow as is indicated by the NDVI imagery. Melt onset over sea ice does not commence until the first week in June north of Alaska, and not until late June north of Siberia. Under these conditions, the pack does not retreat very far north of the coastlines in September leaving stretches of the Siberian coast ice bound.

In contrast, Figure 8b composites four recent years of extreme minimum ice extent. During spring of these years the BSA is poorly defined. Instead, a ridge of high pressure persists over eastern Alaska and the AL is shifted westward. This pattern sets up a strong west-to-east gradient in the pressure field that favors the transport of warm, Pacific air northward (indicated by the red vectors). By late May, Pacific air is further warmed as it flows over bare (low albedo) tundra being irradiated continuously by intense sunlight. This further contributes to an early onset of melt over sea ice. An early, and thus prolonged, melt season amplifies late summer ice retreat, especially in the western Arctic where the ice pack has become younger and thinner.

Linkages to the disposition of the BSA described above suggest that regional scale circulation patterns influence broad scale mechanisms and feedbacks that modulate snow cover and sea ice conditions in the western Arctic. Concerns arise as to whether or not recent trends resulting from these compounding positive feedbacks are manifestations of natural, low-frequency oscillations, or are anthropogenically forced. Will these mechanisms become self-propagating if the global temperature continues to rise? Answers to these questions have important ecological and cultural implications on a pan-Arctic scale. The following historical perspective casts some light on these questions.

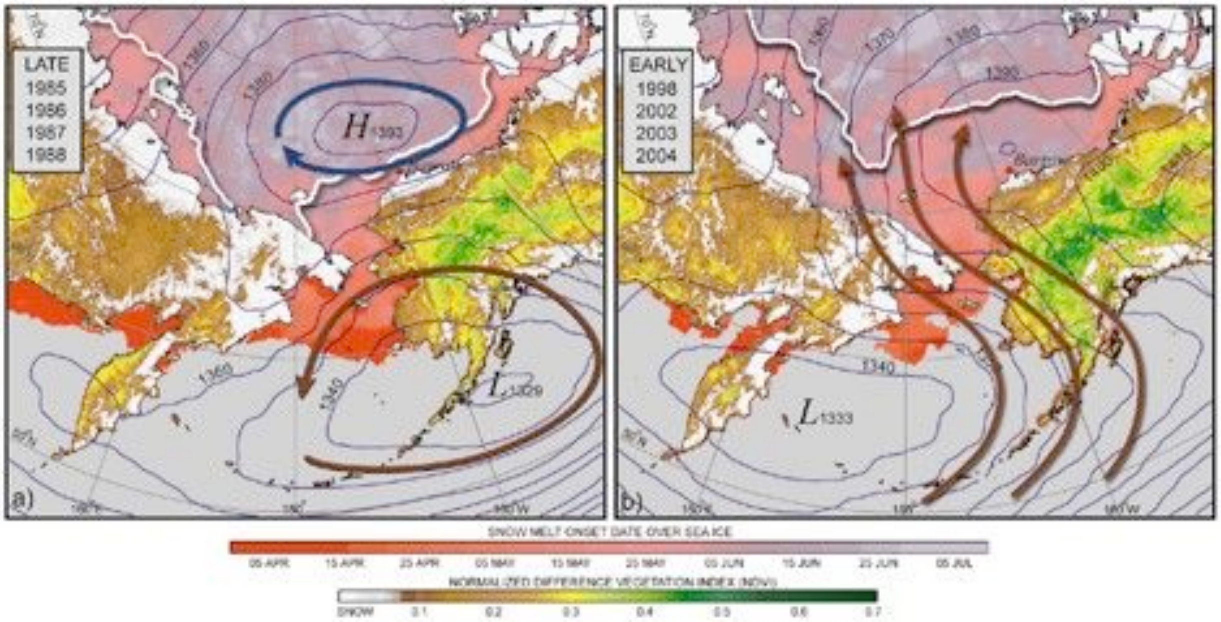

Fig. 8. Environmental conditions over the western Arctic averaged for years with (a) minimum and (b) maximum sea ice retreat. The extent of late summer ice retreat, defined as the southern limit of >50% mean ice concentration during late September, is shown as a bold white line. Thin blue lines depict 10 m contours of mean March–May 850 hPa geopotential heights from the NCEP/NCAR 40-year Reanalysis Project. Generalized circulation patterns are shown with bold vectors. Mean melt onset dates over sea ice are color-shaded for areas where ice concentrations averaged >50% during the second half of May. Vegetation greenness is depicted by the mean maximum NDVI also during tha last two weeks in May, derived from GIMMS NDVI-d and NDVI-n16 datasets [from Stone et al., 2005].

Update and Historical Perspective on the Date of Snowmelt at Barrow

The record of Barrow melt date has been updated through 2006 using the same criteria described in Stone et al. (2002), combining it with recently released historical data from NCDC. The pre-1948 daily cooperative station data were obtained from the NCDC Climate Data Online (CDO) system under its Climate Data Modernization Program. For Barrow some records, including snow depth measurements, extend back to the early 1900s from which preliminary analysis of the melt dates were made. Figure 9 presents an analysis of all past and recent determinations of melt date for Barrow, fitted linearly to evaluate trends. Because recent years, 2004-2006, have been moderately late years of melt and there were several years during the mid 1920s to late 1930s of early melt, the regression shows no statistical significance, contrary to the post-1940 analysis presented in Figure 7. The 1920s-1930s reveal as much variability as observed from 1990 to 2002 and include years of very early melting of the snow pack at Barrow. Unfortunately, data previous to the establishment of the National Weather Station at Barrow in 1921 are practically non-existent, making conclusions somewhat speculative. There appears, however, to be a precedent for the extreme years of early melt that occurred beginning in 1990, years that gave rise to a significant trend when considering only the period 1941 to present. This perspective needs further verification and explanation because it has bearing on how we interpret recent variations in sea ice concentration, which has been shown to correlate with snow cycles through dynamic and thermodynamic processes described above.

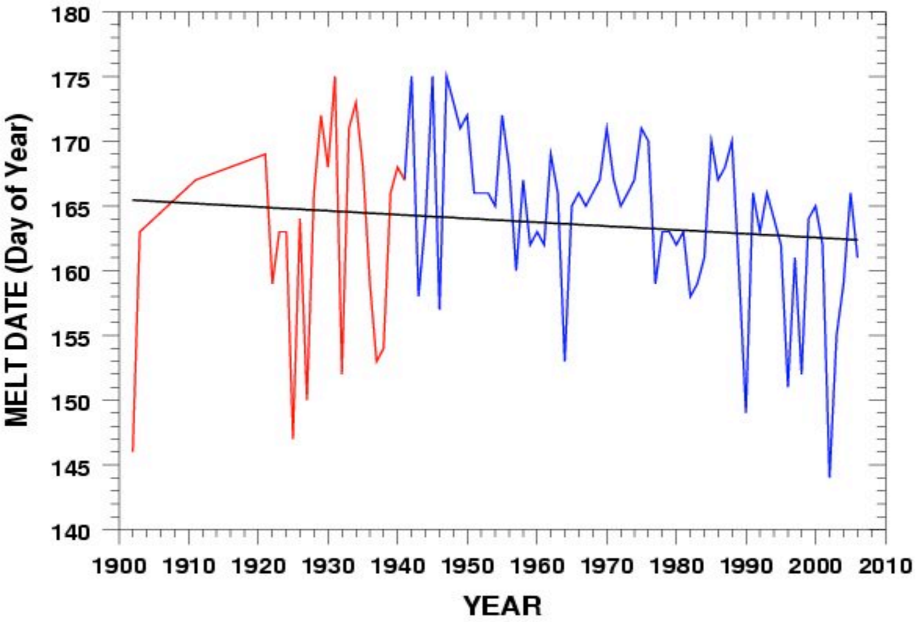

Fig. 9. Update and preliminary analysis of the historical (pre-1941) Barrow melt date time series derived from snow depth and proxy data provided through NCDC Climate Data Online. Inclusion of the earlier and most recent data suggest there is no statistically significant trend as previously documented.

Incursions and Impact of Asian Dust Over Northern Alaska

Using an assimilation of data collected at the CMDL Barrow Observatory (BRW), the direct effects of atmospheric aerosols on the surface radiation budget are being carefully monitored. In the past, the focus has been on "Arctic Haze" that is annually transported from Eurasia to BRW each spring. Analyses reveal incursions of Asian Dust as well. Spectral aerosol optical depth (AOD) measurements are used to differentiate dust from haze, whereby dust typically contains larger particles and is often of higher optical depth. Because polar atmospheres are generally very clean, even small increases in aerosol concentrations can perturb the radiometric structure of the atmosphere and thus the surface energy balance. Using an assimilation of data products available from BRW, the climate impact of different types of aerosols can be quantified as described below (details are given in Schnell et al., 2004, and Stone et al., 2005).

During spring 2002, massive dust storms occurring in the Gobi Desert region of Mongolia lofted dust into the atmosphere that was transported eastward in a broad plume that reached the continental U.S. Some of this dust was blown over northern Alaska, passing over BRW. With the current complement of instrumentation at BRW it is now possible to track these events, monitor their physical properties, and derive or infer something about their optical and microphysical characteristics. For instance, the addition of a tracking sunphotometer system in 2000 has enabled quantification of AOD, while spectral signatures give relative particle size. In situ aerosol sampling at the surface can be used to investigate light scattering by aerosol particles from which fundamental optical properties can be derived, and particle analyses reveal chemical composition to fingerprint source regions. Dust layers are clearly visible in lidar profiles provided DOE ARM. Back trajectory analyses complement or substitute for chemical fingerprinting to determine source regions with some confidence. Finally, the suite of radiometers at the station yields an accurate time series of flux measurements from which the radiative forcing by aerosols can be estimated.

Results show that when dust is present in the Arctic atmosphere, the surface tends to cool. Model results generally corroborate the empirical findings, giving credence to the use of surface radiation measurements for evaluating the climatic impact of aerosols in polar regions. In this particular case, for a modest optical depth in the visible spectrum, AOD (500 nm) = 0.15, this amounts to a negative forcing of about 5 W m^{-2} averaged over the diurnal cycle, a cooling effect that is greater than the warming estimated from a doubling of CO_2.

Extinction by aerosols in the atmosphere is greatest in the visible portion of the solar spectrum. Thus, solar irradiance reaching the surface diminishes measurably with increasing turbidity. It is straightforward to calculate the NET shortwave (SW) flux (NETSW = SWdown - SWup) at the surface and evaluate changes as a function of optical depth. When turbid conditions are compared with pristine periods, a measure of the direct radiative forcing by the intervening aerosol layers can be estimated. This quantity is referred to here as the Direct Aerosol Radiative Forcing (*DARF*). Similarly, radiative transfer theory can be used to calculate *DARF*. This was done to enable a comparison of model and empirical results, a first attempt at such a "closure experiment" for an Arctic location characterized by high surface albedo (82-84%) and low solar angles. MODTRAN5™, the most recent version of a radiative transfer code developed by the Air Force, was used in this study.

Figure 10 compares the empirical and model results for three distinct solar zenith angles. These results illustrate the significant variation in *DARF* over a typical diurnal cycle for April at BRW. *DARF* is defined simply as the change in NETSW radiation per unit optical depth; i.e., the slope of each regression. Negative slopes indicate cooling at the surface when dust is present in the atmosphere above BRW. Table 1 compares the independent results of *DARF* estimated for each zenith angle.

Table 1. Direct Aerosol Radiative Forcing (*DARF*) for the April 2002 dust episode at Barrow, Alaska. Units are Wm^{-2} unit AOD^{-1}. Negative values indicate cooling at the surface.

Zenith angle	**81°**	**75°**	**62°**
Observed	-16.1	-30.2	-37.8*
Modeled	-15.9	-28.2	-35.0

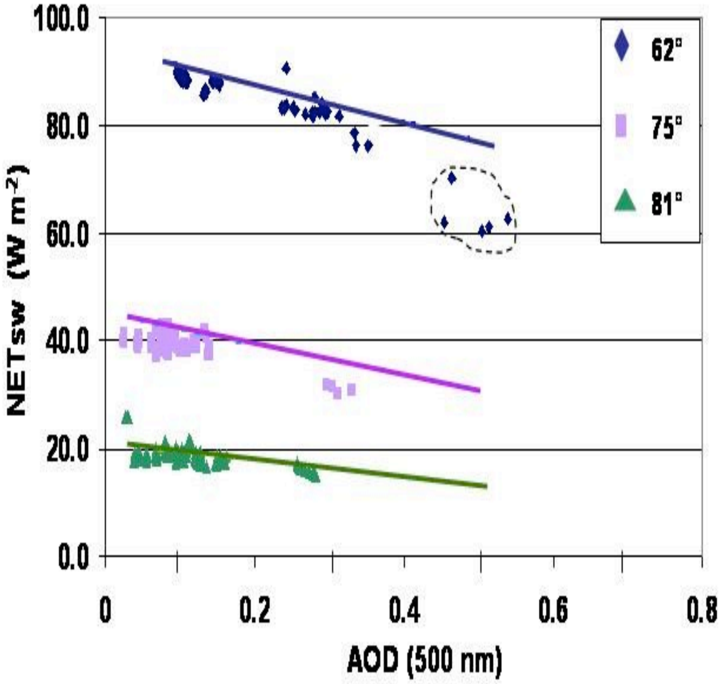

Fig. 10**.** Comparison of measured and simulated surface net shortwave irradiance as a function of visible (500 nm) aerosol optical depth during an Asian dust event at Barrow Observatory, April 2002. Symbols represent one-minute measurements and solid lines the results from MODTRAN™ fitted using linear regression for zenith angles indicated at the upper right. The circled (suspect) points were not used in the 62° analysis for purposes of computing *DARF* empirically.

Radiative Forcing by Boreal Smoke in the Arctic

In the above example, MODTRAN™ simulated the empirical analyses well, especially in terms of *DARF* (the slope of the regressions as listed Table 1). In this case we find that dust from the Gobi has a cooling effect on the snow-covered surface at Barrow in spring.

During summer 2004 forest fires raged in eastern Alaska and western Canada for weeks, burning over 12 million acres of boreal forest (Stohl, et al., 2006). In early July 2004 a plume of smoke from these fires passed over Barrow, enabling an analysis similar to that presented above for Asian Dust. Again, the agreement between empirical and MODTRAN™ results were good, providing “closure” over a range of zenith angles and giving further credence to the model. On this basis it was possible to evaluate the direct aerosol radiative forcing (*DARF*) for hypothetical surfaces for which no data yet exists. The analysis (unpublished) shows a very significant dependence of *DARF* on surface albedo as determined from simulations made for boreal smoke. This is illustrated in Figure 11, which shows only model results for a range of surface conditions (albedos) indicated in the inset. The optical properties of smoke were held constant, as was the zenith angle of 65°, while albedo was prescribed for each hypothetical surface.

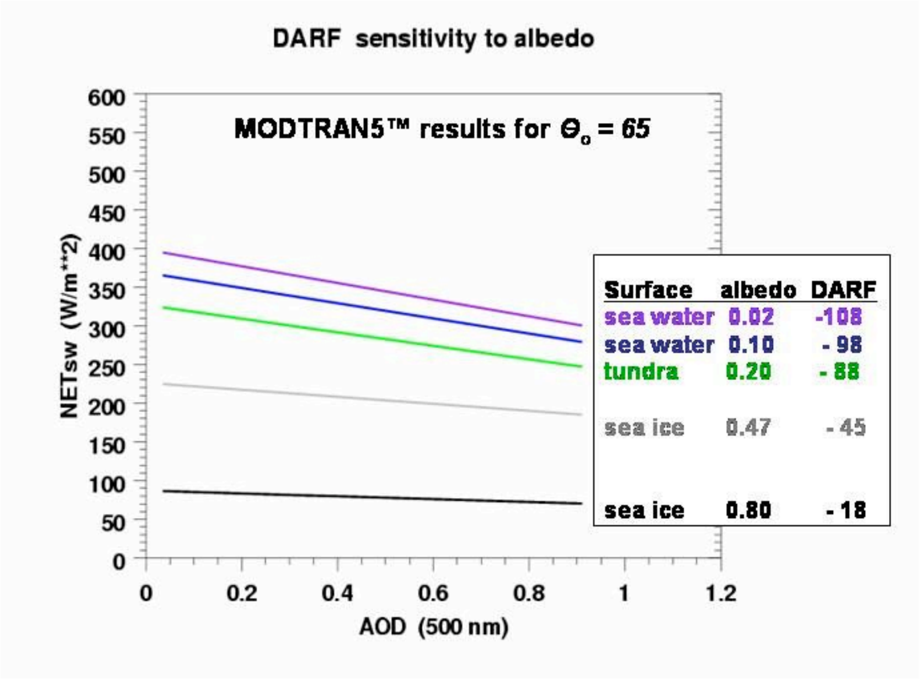

Surface	albedo	DARF
sea water	0.02	-108
sea water	0.10	- 98
tundra	0.20	- 88
sea ice	0.47	- 45
sea ice	0.80	- 18

Fig. 11. Simulations of the direct aerosol radiative forcing (*DARF*) of boreal smoke for differing surface albedo representing a range of Arctic conditions. Each curve represents a different hypothetical surface. A solar zenith angle of 65^o was prescribed, the approximate daily average for Barrow at the beginning of summer. Values of *DARF* are given in the table (inset).

It is very apparent that forcing by smoke varies dramatically as a function of surface type (albedo) for fixed zenith angle. In turn, the surface radiation balance will be variably affected by aerosol loading as surface conditions change in the spring-summer transition period. The factor of 5-6 increase in forcing as snow covered sea ice (albedo ≈ 0.8) melts and exposes dark water (albedo ≈ 0.02 - 0.10) has significant climatic consequences considering this is a negative feedback (cooling effect) that counters the effect of greenhouse warming. This is especially true in summer when snow and ice cover are at their minimal extents and *DARF* is large. Valid impact assessments are not possible until the convolution of aerosol composition (type), solar geometry, and surface albedo is accounted for, all of which vary spatially and temporally. While haze, dust and smoke occur only episodically in the Arctic, their cumulative radiative impact is probably significant and any perturbation in environmental conditions and/or atmospheric dynamics that increases atmospheric opacity must be monitored. Stohl, et al. (2006) illustrate nicely how extensive and prolonged the effects of forest fires can be as smoke emitted over several weeks spread over vast regions over the Arctic during summer 2004. Should the Arctic atmosphere become more turbid, projections of enhanced warming in the Arctic may be overestimated due to a negative feedback. On the other hand, high concentrations of carbonaceous particles that absorb sunlight could lead to a positive feedback. More complicated and of greater climatic importance is the *indirect* effect of aerosols on cloud properties as pertaining to radiative effects. Much more data and model simulations must be analyzed before we fully understand the climatic impacts of polar aerosols. To this end we have begun to compile data to characterize the various aerosols that influence Arctic climate, the first step in developing a realistic aerosol climatology needed for climate assessments and to improve parameterization of their effects.

Characterization of Polar Aerosols

The photometric data used to evaluate the radiative forcing by transient layers of dust, haze and smoke have also been useful for characterizing these different aerosol types. As data become available they are examined for spectral signatures. From such analyses a climatology of Polar aerosols will be produced. Also, spectral signatures can be used as a basis for parameterizing or identifying various aerosols that influence climate. We are finding that different types of aerosol can be identified as having certain behavior associated with their relative size, where particle size is inversely proportional to a parameter referred to as the Angstrom Exponent (*AE*). *AE* is quantified as the negative slope of the spectrally varying aerosol optical depth (*AOD*) when plotted on a log scale (Stone, 2002). Figure 12 illustrates how different aerosols can be classified by plotting their *AE* (derived from a pair of wavelengths) as a function of AOD at 500 nm. Points falling near the bottom and to the right have larger particle size and greater opacity than at the upper left. We find that pristine conditions at South Pole (Spole) have the lowest values of AOD and the particles are smallest, whereas dust particles tend to be large and more opaque. Smoke from boreal forest fires tend to be invariant in size while having a wide range of optical depth. Such knowledge will be useful for improving parameterizations of aerosols for climate studies.

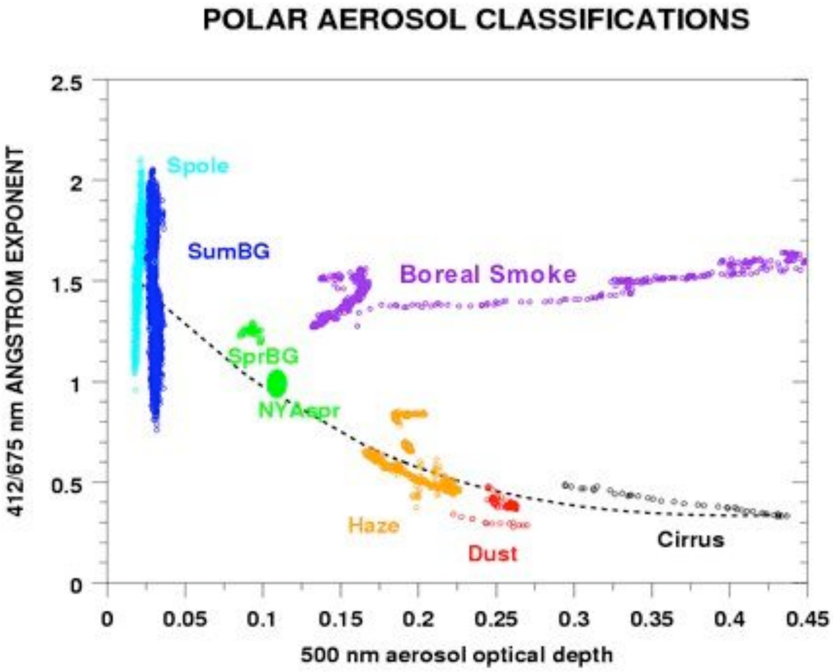

Fig. 12. Plot of Ångström exponents as a function of 500 nm aerosol optical depth. Clusters of points correspond to one minute data with exception of points labeled NYAspr, which represents a mean for Ny-Alesund for spring. The dashed curve is a best fit of all the data, excluding boreal smoke. Particle size is inversely related to the Ångström exponent. From left to right, Spole represents pristine conditions at South Pole with other clusters representing summer and spring background (BG) conditions, Arctic haze, Asian dust, and cirrus cloud at Barrow, AK, respectively. Smoke, made up of small particles, has a distinctive signature that is invariant over a range of AOD.

Cloud and Surface Temperature Studies

The cloud and surface temperature studies have several objectives; (1) to begin developing statistics on the annual and interannual variability of cloud properties over Barrow as determined directly from ground sensors, (2) to compare the ground sensor data to satellite-based cloud data sets to determine a sense of the confidence that could be placed in multi-decadal, Arctic-wide satellite measurements of clouds, (3) to determine how clouds might impact satellite detection of other environmental parameters such as surface temperature, (4) to take a preliminary look at trends, and (5) to develop a database that would be useful for model validation, parameterization development, and other studies of Arctic clouds.

Cloud Studies using Radar Data in Barrow

The surface data from Barrow, Alaska, including measurements from cloud radar, microwave radiometer, and soundings, were used to develop information on cloud properties for the period 1998 - 2003. This was not a smooth procedure. The radar data in Barrow has been discontinuous with unfortunate and frequent gaps during spring and summer, impacting the reliability of the statistical studies. Also, careful examination of the annual radar reflectivity statistics and individual examination of snowfall cases (when minimum reflectivity values are considered to be well known) raised concerns that there have been extended periods during which the radar reflectivities have been biased low. Some of these periods of compromised data have known causes (water in the waveguide) and others have not yet had identified hardware or software processing problems. NOAA/PSD has alerted DOE/ARM to the problem and there is a discussion about radar reprocessing and flagging, since the incorrect reflectivities will result in cascading errors in the calculation of cloud parameters such as optical depth, ice and liquid water contents and crystal/droplet sizes. During this period there was also a significant delay with data processing due to an upgrade in radar processor hardware (in 2004) that preceded the development of software to handle the reformatted data streams.

The present uncertainties in the radar data have delayed some of the quantitative cloud property statistics studies, and for the NOAA SEARCH activities the focus was on cloud fraction/presence studies (which are not expected to be significantly affected) and non-quantitative cloud optical depth studies. Since these radar issues affecting the calculation of cloud microphysical properties have not yet been resolved, the published studies on the annual variability of cloud microphysical properties have focused on the SHEBA data sets (Shupe et al., 2005), and more qualitative studies were conducted with the Barrow data. One of the primary results of the cloud property studies from SHEBA that have been corroborated non-quantitatively with the Barrow data is that layers of liquid water in Arctic clouds appear to occur frequently throughout the year, often persisting for long periods. This information has prompted focused mixed-phase cloud studies such as MPACE (Mixed Phase Arctic Cloud Experiment) conducted by DOE with a contribution from the NOAA/SEARCH program.

The development of the new radar processors has resulted in recording of full radar spectra. The radar spectra have been used to develop techniques to determine cloud phase (Shupe et al., 2004b). These techniques, both stand-alone and in combination with more standard multi-instrument lidar/radiometer cloud phase retrievals, are valuable in the on-going cloud studies at the Intensive Observatories, since phase has been identified as a primary cloud property that controls cloud radiative properties.

Relative Importance of Cloud Fraction and Cloud Optical Depth

Since clouds have been recognized as a major factor in the Arctic climate system, a number of cloud fraction/presence studies have been done to determine if there are increasing or decreasing trends in cloudiness. The determination of accurate cloud fraction in the Arctic is both non-trivial and a necessary precursor to derivation of any other cloud properties. However, the question was posed in this study as to whether or not cloud fraction had a strong relation to actual cloud forcing, or if cloud optical depth, which is computationally related to liquid and ice water path, would be a more appropriate parameter with which to assess cloud impacts.

Studies were conducted with SHEBA data to determine factors controlling cloud optical depth and the resulting effects on surface cloud forcing. Zuidema et al. (2005) demonstrated that by an order of magnitude, the primary contribution to cloud optical depth in a cloud with mixed ice and liquid layers is from super cooled liquid layers, even though they were often geometrically much thinner than the ice layers. Shupe et al. (2004) further showed that clouds with liquid have a statistically much larger effect on surface cloud forcing than clouds with ice only. It was concluded that geometrically thick (several km) ice clouds might be radiatively less significant than very thin (100s of meters) liquid layers. These results initiated the comparison of not only cloud fraction but also cloud optical depth between the Barrow surface sensors and several satellite system/retrieval techniques (Figure 13). The satellite cloud sensors/retrievals include the AVHRR/APP-x, MODIS/CERES-TEAM, TOVS/Polar Pathfinder (Path-P), and AVHRR/PATMOS-x. The results indicate that while the satellite sensors seem to be doing a reasonable job with detecting cloud fraction, cloud optical depth may be more problematic, especially for the older sensors (AVHRR), which have fewer spectral channels on which to base retrievals.

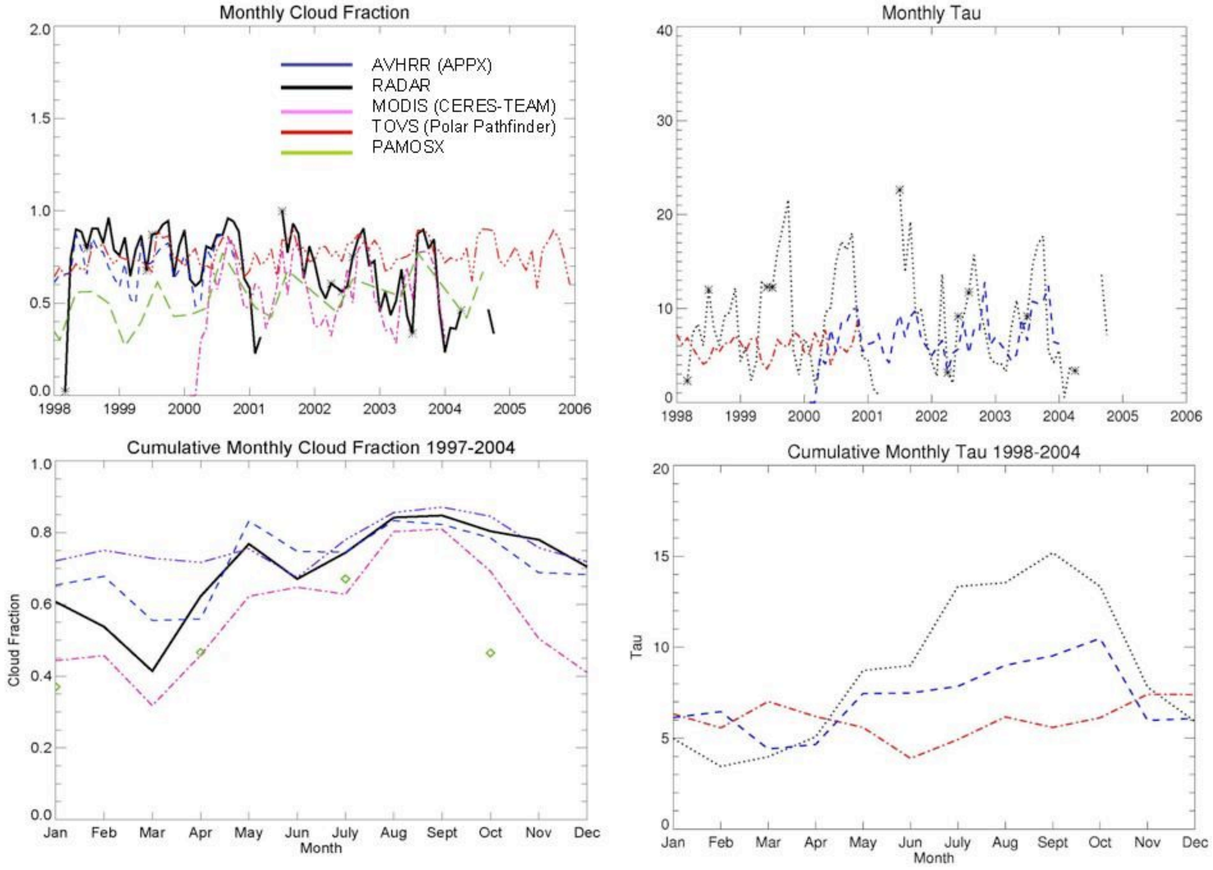

Fig. 13. Comparison of radar cloud fraction and optical depth with APP-x, MODIS-CERES TEAM, TOVS Path-P, and PATMOS-x. Monthly averages in top panels and cumulative monthly averages in bottom panels.

Cloud Impacts on Detection of Surface Temperatures

To investigate the impacts of clouds on the estimation of surface temperature from satellites, comparisons were made between the surface temperatures at Barrow, Tiksi, Alert and Eureka and those derived from the APP-x data set for the period 1982 - 2000. These are the stations where the NOAA SEARCH program is conducting and expanding intensive surface observations. Results were also partitioned by cloud amount, for cloud fractions less than 0.8, 0.6, 0.4, and 0.2. Figure 14 shows the results for Alert and Barrow. At Alert (Figure 14 left panel), the APP-x surface temperatures are warmer than the observed surface temperatures in winter and colder by about 4 degrees in the late spring, summer and early fall. Comparing surface temperature difference for different cloud fraction subsets appears to increase the difference (and in the case of January to completely change the sign) but also results in a constant offset of 4 degrees throughout the year. This difference is not necessarily an error but is more likely the result of (a) the difference between the satellite-derived “skin” temperature and the meteorological station measurements being made around 2 m above the surface, and (b) the large area over which the satellite results were averaged (125 x 125 km), which undoubtedly includes some coverage of the adjacent ocean. Skin and air temperature differences can be large in the presence of steep surface-based inversions.

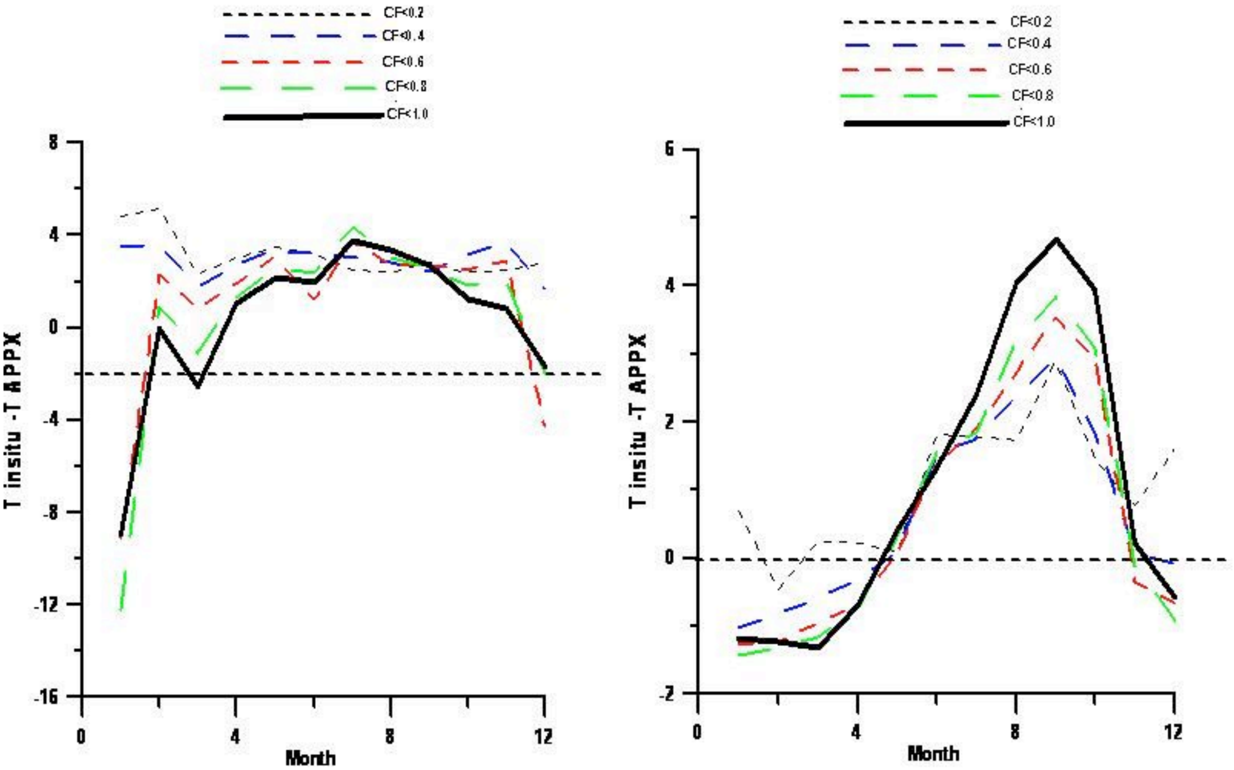

Fig. 14. Mean monthly difference in surface temperature (surface – APP-x) for Alert (left panel) and Barrow (right panel)

Corresponding results of the mean monthly differences between the APP-x and surface temperatures for Barrow have a similar pattern, i.e., higher APP-x temperatures in winter and lower APP-x temperatures in summer. However, there are differences in the shape of the annual cycle; Barrow shows more of a month-to-month change than Alert. This is consistent with the fact that Barrow is at a lower latitude than Alert (71 vs. 82 degrees) and there is larger variation in seasonal solar zenith angle that may be creating a more seasonally driven bias in the retrieval techniques. Examining the differences as a function of cloud fraction indicates that during clear sky conditions the temperature differences at Barrow are close to 0 in winter and are reduced in summer, although the effect of a possible difference in the measurement of skin temperature and surface air temperature and a persistent inversion is apparent. It should be noted that statistically Barrow is much cloudier than Alert, so the satellite-derived surface temperatures may be less reliable as a result.

The temperature differences between APP-x and the surface measurements were examined more closely for individual months and times. Figure 15 shows the monthly difference for March and July in Alert at both 0400 LST and 1400 LST, the two APP-x composite times. The monthly temperature differences during July show a very constant offset of about 5 degrees and it appears that the calculation of trends from the surface and APP-x data sets would yield similar results. In March, differences are generally less. However, the earlier part of the data record (prior to 1980) shows significantly larger differences indicating that some of the earlier sensors may have had factors that impacted winter time Arctic temperature retrievals in particular. There do not appear to be large differences between 0400 and 1400 for March and July.

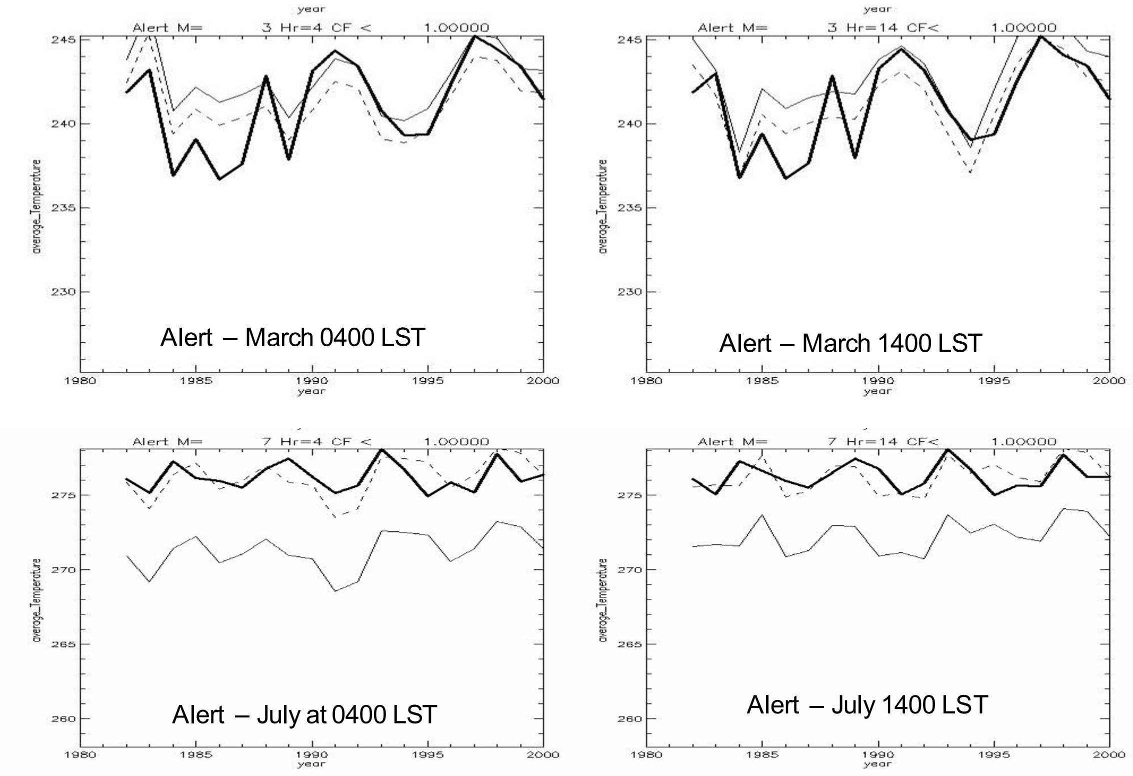

Solid Line – Surface Grey Line – APPX Dashed Line – “Corrected” APPX

Fig. 15. Monthly temperature differences at Alert for March (upper panels) and July (lower panels) at 0400 LST (left panels) and 1400 LST (right panels).

Trends at the Intensive Observatory Sites

Although the previous sections have addressed some unresolved issues about the agreement between absolute values of surface temperature, optical depth, and cloud fraction, and the APP-x data sets are not considered long enough for accurate trend analysis, a cautious preliminary examination of the changes in these parameters was examined for satellite pixels close to Barrow, Alert, Tiksi and Eureka. One particular puzzle that seems to be emerging in Arctic climate studies is that although clouds generally have a warming effect on the Arctic surface, a number of recent studies have shown that cloud fractions appear to be decreasing during part of the year, even though the Arctic is warming overall.

There are two possible hypotheses that are being investigated at present. The first hypothesis is that as sea ice extent is decreasing and the amount of bare ground is increasing due to reduced snow cover, the surface background is becoming darker and warmer. This darker background may be affecting the retrievals of cloud fraction. The second hypothesis is driven by the example shown in Figure 16 of the optical depth and cloud fraction changes at Alert for the winter season. The figures show that in Alert, the decrease in cloud fraction appears to be accompanied by an increase in cloud optical depth, at least in the APP-x data set. This is further supported by the results suggesting that cloud optical depth (a measure of total water path, particularly liquid water path) is a better measure of the cloud radiative forcing effects then the cloud fraction.

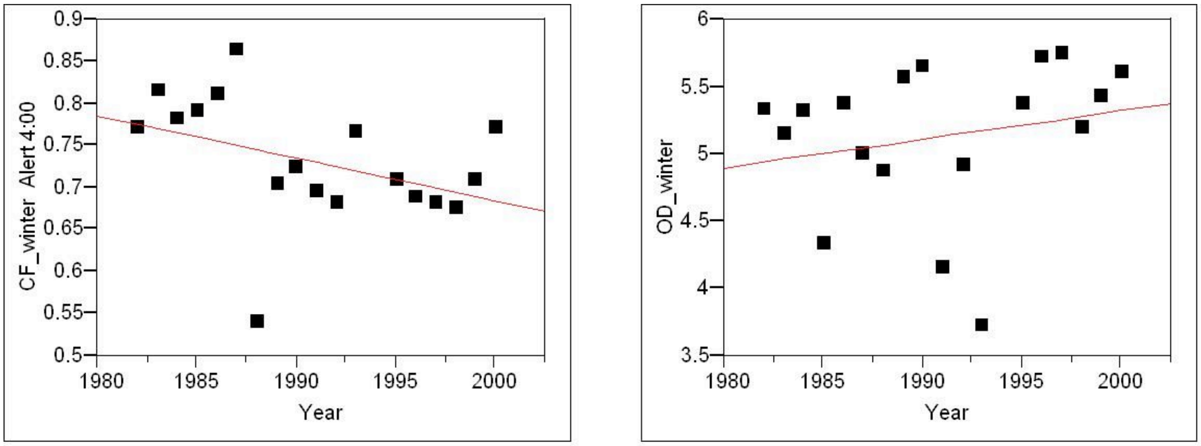

Fig. 16. Annual average cloud fraction (left panel) and cloud optical depth (right panel) at Alert from APP-x.

Table 1 shows a summary of the changes in surface temperatures, cloud optical depth and cloud fraction for the winter and summer seasons in Barrow, Eureka, Alert and Tiksi. Interestingly, the surface temperature changes are almost all positive, indicating increasing temperatures for all sites. The cloud fraction increases in summer and decreases in winter at all sites (but with an average of decreasing cloudiness); optical depth generally increases. These results underscore the need for careful averaging so that signals are not lost and also the necessity of identifying the cloud properties that can be used as climate change indexes.

TEMPERATURE CHANGE 1982 through 2000

	1982-2000 APP-x	1982-2001 Surface	
Barrow Winter	1.24 ±1.26	+2.300	
Barrow Summer	+1.01 ±0.4	+1.532	
Alert Winter	0.88 ±1.13	-0.076 ±0.75	
Alert Summer	+1.19 ± 0.67	+0.21 ±1.12	
Eureka Winter	+1.99 ±1.26	+0.96 ±01.3	
Eureka Summer	+1.517 ±1.55	+0.59 ±1.16	
Tiksi Winter	+0.20 ±1.33	Surface ends 1990	
Tiksi Summer	+1.3 ±1.3	Surface ends 1990	

OPTICAL DEPTH CHANGE 1982 through 2000

	4:00 hours	14:00 hours	Average
Barrow Winter	0.7	0.43	0.59 ±0.37
Barrow Summer	0.77	0.89	0.855 ±0.31
Alert Winter	0.43	0.38	0.18 ±0.54
Alert Summer	-0.34	-0.054	0.12 ±0.32
Eureka Winter	1.13	0.99	1.062 ±0.39
Eureka Summer	-0.36	0.29	-0.091 ±0.27
Tiksi Winter	-0.072	0.054	-0.0043 ±0.4
Tiksi Summer	0.34	-0.054	0.11 ±0.4

CLOUD FRACTION CHANGE 1982 through 2000 linear fit error approx ±0.05

	4:00 hours	14:00 hours	Average
Barrow Winter	-0.085	-0.052	-0.068 ±0.047
Barrow Summer	0.065	0.072	0.072 ±0.039
Alert Winter	-0.092	-0.117	-0.104 ±0.07
Alert Summer	0.029	0.040	0.034 ±0.31
Eureka Winter	-0.088	-0.100	-0.094 ±0.076
Eureka Summer	0.070	0.077	0.054 ±0.033
Tiksi Winter	-0.15	-0.036	-0.094 ±0.065
Tiksi Summer	0.009	0.029	0.019 ±0.038

Data Products

A three-year (2000, 2001, 2002) cloud microphysical dataset based on radar and radiometric data from the North Slope of Alaska, and for the SHEBA year (Nov 1997-Nov 1998), was released on CD and sent to an extensive mailing list of Arctic researchers. In addition, three more years of NSA data (1998, 1999, and 2003) have been processed, and it is anticipated that a second CD release will occur in FY2004. Data from 1998 at NSA has been "lost" to the ARM program since collection. Discovery of backup tapes at ETL for this period and subsequent processing is especially fortuitous as this period provides overlap with the SHEBA data sets. Descriptions of these data sets and products and updated data sets can also be viewed via the Web at: http://www.etl.noaa.gov/arctic (see data links on left bar).

The APP-x dataset, consisting of retrieved surface properties, cloud properties and radiative fluxes for the area north of 60^{o}N, was processed through 2004. Parameters are available on twice-daily and monthly mean time scales. The data and read routines are available to the public at http://stratus.ssec.wisc.edu.

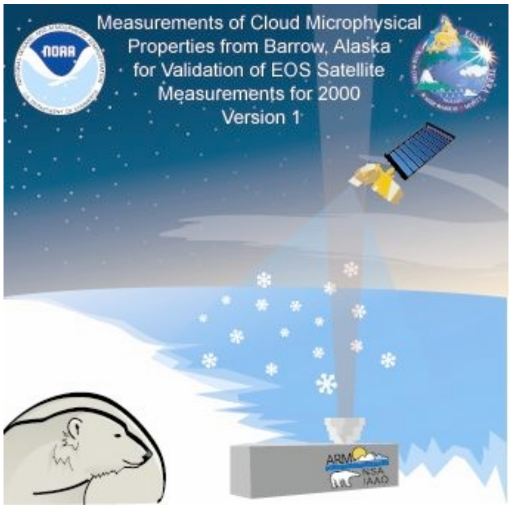

Measurements of Cloud Microphysical Properties from Barrow, Alaska for Validation of EOS Satellite Measurements for 2000
Version 1

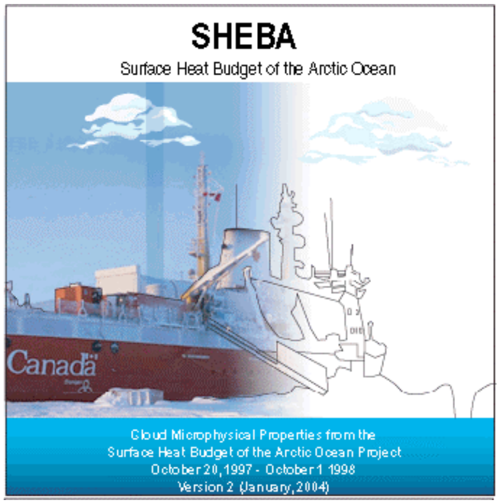

SHEBA
Surface Heat Budget of the Arctic Ocean

Cloud Microphysical Properties from the Surface Heat Budget of the Arctic Ocean Project
October 20, 1997 - October 1 1998
Version 2 (January, 2004)

Publications

Journal Papers

Chapin, F.S., M. Sturm, M.C. Serreze, J.P. McFadden, J.R. Key, A.H. Lloyd, A.D. McGuire, T.S. Rupp, A.H. Lynch, J.P. Schimel, J. Beringer, H.E. Epstein, L.D. Hinzman, G. Jia, C.-L. Ping, K. Tape, W.L. Chapman, E. Euskirchen, C.D.C. Thompson, J.M. Welker, and D.A. Walker, 2005, Role of land surface changes in Arctic summer warming, Science, vol. 310, doi: 10.1126/science.1117368, October 28.

Dutton, E.G., D.W. Nelson, R.S. Stone, D. Longenecker, G. Carbaugh, J.M. Harris, and J.Wendell; Decadal Variations in Surface Solar Irradiance as Observed in a Globally Remote Network, *J. Geophys. Res.,* in press, 2006.

Dutton, E. G., A. Farhadi, R. S. Stone, C. N. Long, and D. W. Nelson (2004), Long-term variations in the occurrence and effective solar transmission of clouds as determined from surface-based total irradiance observations, J. Geophys. Res., 109, D03204, doi:10.1029/2003JD003568.

Francis, J.A., E. Hunter, J. Key, and X. Wang, 2005, Clues to variability in Arctic minimum sea ice extent, Geophys. Res. Letters, vol. 32, L21501, doi: 10.1029/2005GL024376, November 15.

Hinzman, L., N. Bettez, W.R. Bolton, F. S. Chapin, M. Dyurgerov, C. Fastie, B. Griffith, R.D. Hollister, A. Hope, H.P. Huntington, A. Jensen, G.J. Jia, T. Jorgenson, D.L. Kane, D.R. Klein, G. Kofinas, A. Lynch, A. Lloyd, A. D. McGuire, F. Nelson, W. C. Oechel, T. Osterkamp, C. Racine, V. Romanovsky, R. Stone, D. Stow, M. Sturm, C.E. Tweedie, G. Vourlitis, M.Walker, D. Walker, P. J. Webber, J. Welker, K. Winker, K. Yoshikawa; Evidence and Implications of Recent Climate Change in Northern Alaska and Other Arctic Regions, *Climate Change*, Vol. 72, No. 3, 251 – 298, DOI: 10.1007/s10584-005-5352-2, 2005.

Liu, Y., J. Key, R. Frey, S. Ackerman, and W.P. Menzel, 2004, Nighttime polar cloud detection with MODIS, J. Appl. Meteorol., submitted (January 2004).

Liu, Y., J. Key, A. Schweiger, and J. Francis, 2006, Characteristics of satellite-derived clear-sky atmospheric temperature inversion strength in the Arctic, 1980-1996, J. Climate, 19(19), 4902-4913.

Liu, Y., J. Key, and X. Wang, 2006, The Influence of Changes in Cloud Cover on Recent Surface Temperature Trends in the Arctic, J. Climate, submitted (September 2006).

Overpeck, J.T., M. Sturm, J.A. Francis, D.K. Perovich, M.C. Serreze, R. Benner, E.C. Carmack, F.S. Chapin III, S.C. Gerlach, L.C. Hamilton, L.D. Hinzman, M. Holland, H.P. Huntington, J.R. Key, A.H. Lloyd, G.M. MacDonald, J. McFadden, D. Noone, T.D. Prowse, P. Schlosser, and C. Vörösmarty, 2005, Arctic system on trajectory to new, Seasonally ice-free state, EOS, 86(34), 309-314.

Shupe, M.D., and J.M. Intrieri, 2004a: Cloud radiative forcing of the Arctic surface: The influence of cloud properties, surface albedo, and solar zenith angle. J. Climate, 17, 616-628

Shupe, M.D., P. Kollias, S.Y. Matrosov, and T.L. Schneider, 2004b: Deriving mixed-phase cloud properties from Doppler radar spectra. J. Atmos. Ocean. Tech., 21, 660-670.

Shupe, M.D., T. Uttal, and S.Y. Matrosov, 2005: Arctic cloud microphysics retrievals from surface-based remote sensors at SHEBA. J. Appl. Meteor., 44, 1544-1562.

Stohl, A., E Andrews, J. F. Burkhart, C. Forster, D. Kowal, C. Lunder, T. Mefford, J. A. Ogren, S. Sharma, N. Spichtinger, K. Stebel, R. Stone, J. Strom, K. Torseth, and C. Wehrli; Pan-Arctic enhancements of light absorbing aerosol concentrations due to North American boreal forest fires during summer 2004, *J. Geophys. Res*., in press, 2006.

Stone, R.S., D. Douglas, G. Belchansky, and S. Drobot; Correlated Declines in Pacific Arctic Snow and Sea Ice Cover, *Arctic Research U.S.*, NSF, Arlington, VA, Vol. 19, 18-25, 2005.

Wang, X. and J. Key, 2003, Recent trends in Arctic surface, cloud, and radiation properties from space, Science, 299(5613), 1725-1728.

Wang, X. and J. Key, 2005, Arctic surface, cloud, and radiation properties based on the AVHRR Polar Pathfinder data set. Part I: Spatial and temporal characteristics, J. Climate, 18(14), 2558-2574.

Wang, X. and J. Key, 2005, Arctic surface, cloud, and radiation properties based on the AVHRR Polar Pathfinder data set. Part II: Recent trends, J. Climate, 18(14), 2575-2593.

Zuidema, P., B. Baker, Y. Han, J. Intrieri, J. Key, P. Lawson, S. Matrosov, M. Shupe, R. Stone, T. Uttal, 2005, An Arctic springtime mixed-phase cloudy boundary layer observed during SHEBA, J. Atmos. Sci., 62, 160-176.

Conference Papers

Stone, R., G. Anderson, E. Andrews, E. Dutton, J. Harris, E. Shettle, and A. Berk; Asian dust signatures at Barrow: observed and simulated, IEEE Workshop on Remote Sensing of Atmospheric Aerosol, An Honorary Workshop for Prof. John A. Reagan, 5-6 April 2005a, University of Arizona, Tucson Arizona, USA, 74-79, 2005. ftp://ftp.cmdl.noaa.gov/pub/betsy/IEEEStoneetal2005.pdf

Stone. R.S., D. C. Douglas, G. I. Belchansky, S. D. Drobot, and J. Harris; CAUSE AND EFFECT OF VARIATIONS IN WESTERN ARCTIC SNOW AND SEA ICE COVER, 8th Conference on Polar Meteorology and Oceanography, 8.3, The 85th AMS Annual Meeting (San Diego, CA), January 2005.

Uttal, T., S. Frisch, X. Wang, J. Key, A. Schweiger, S. Sun-Mack, and P. Minnis, 2005, Comparison of monthly mean cloud fraction and cloud optical depth determined from surface cloud radar, TOVS, AVHRR, and MODIS over Barrow, Alaska, *Proceedings of the 8th Conference on Polar Meteorology and Oceanography*, January 9-13, San Diego.

Uttal, T., S. Frisch, X. Wang, and J. Key, 2004, Long-term observations of cloudiness, radiation, and aerosols with permanent atmospheric observatories, Proceedings of the ACIA International Scientific Symposium “Climate Change in the Arctic”, Reykjavik, Iceland, November 9-12.

Wang, X. and J. Key, 2004, Arctic climate characteristics and recent trends from space, Proceedings of the SPIE International Asia-Pacific Symposium, Honolulu, Hawaii, November 8-12.

Wang, X. and J. Key, 2004, Satellite-derived Arctic climate characteristics and recent trends, Proceedings of *the 13th Conference on Satellite Meteorology and Oceanography*, Norfolk, Virginia, September 20-24.

Uttal, T. Sun-Mack S., P. Minnis and J. Key, 2003: Comparison of Surface AND Satellite Measurements of Arctic Cloud Properties, 7th Conf on Polar Meteorology and Oceanography.

Wang, X. and J. Key, 2003, Recent Arctic climate trends observed from space and the cloud-radiation feedback, *Proceedings of the Seventh Conference on Polar Meteorology and Oceanography*, American Meteorological Society, Hyannis, MA, May 12-16.

Reports

Levinson, D.H., ed.; STATE OF THE CLIMATE IN 2004, *Bulletin of the American Meteorological Society:* Vol. 86, No. 6, pp. S1–S86, doi: 10.1175/BAMS-86-6-Levinson; Section on Sea Ice, Stone et al., 2005**.**

Schnell et al., eds, NOAA/CMDL Summary Report No. 27 2002-2003: Stone: 1. Polar Aerosol Characterizations; 2. Incursions and Impact of Asian Dust Over Northern Alaska, 3. Western Arctic Meltdown Continues, 2004.

Levinson, D. H., and A.M. Waple; State of the Climate in 2003, Bulletin of the American Meteorological Society, vol. 85, Issue 6, pp.881-881, 2004; Sections on Diminishing Sea Ice in the Western Arctic Ocean, and Snow melt; Stone et al., 2004.

Theses

Wang, X. 2003, “Arctic Climate Characteristics and Recent Trends from Space”, Ph.D Dissertation, University of Wisconsin-Madison, December 2003.

Presentations

Persson, O., R. Stone, M. Shupe, and T. Uttal; Surface Energy Budget, Boundary Layer Structure and Synoptic/Orographic Influences at Arctic Climate Observatories for the Study of Environmental Arctic Change (SEARCH), NOAA/ESRL/Global Monitoring Divsion Annual Review, Boulder, CO, April 26-27, 2006.

Persson, O., R. Stone, M. Shupe, and T. Uttal; Investigating Interactions of Surface Energy Budget, Boundary Layer Structure, and Synoptic/Orographic Influences at Climate Monitoring Observatories for the Study of Environmental Arctic Change (SEARCH). Abstracts, European Geophysical Union Meeting, Vienna, Austria, April 2-7, 2006.

Stone, R.S., G. Anderson, E. Andrews, E. Shettle, E. Dutton , A. Stohl, and M. Fromm; A MODTRAN™ Validation Study: Calculations of Radiative Forcing by Boreal Forest Fire Smoke in the Arctic, 28th Review of Atmospheric Transmission Models, Museum of Our National Heritage, Lexington, Massachusetts, 14-15 June 2006.

Stone, R.S., G. Anderson, E. Andrews, E. Shettle, E. Dutton , A. Stohl, M. Fromm; Smoke Screens

Arctic Warming, NOAA/ESRL/Global Monitoring Divsion 2006 Annual Review, Boulder, CO, April 26-27, 2006.

Stone, R.S., , E. Andrews, S. Sharma, R. Leaitch, T. Uttal, J. Wendell, D. Longenecker, B. McArthur, E. Dutton, J.A. Ogren, P. Sheridan, C. Audette, A. Platt, D. Nelson and J. Treadwell; Enhanced Climate Monitoring Activities at ALERT, Canada; Canada and the U.S. Partner in the Study of Environmental Arctic Change (SEARCH), NOAA Climate Monitoring and Diagnostics Laboratory 2005 Annual Meeting, Boulder, CO, April 20-21, 2005.

Stone, R., G. Anderson, E. Andrews, E. Dutton, J. Harris, E. Shettle, and A. Berk; Asian dust signatures at Barrow: observed and simulated, IEEE Workshop on Remote Sensing of Atmospheric Aerosol, An Honorary Workshop for Prof. John A. Reagan, 5-6 April 2005, University of Arizona, Tucson, Arizona, 74-79, 2005.

Stone. R.S., D. C. Douglas, G. I. Belchansky, S. D. Drobot, and J. Harris; CAUSE AND EFFECT OF VARIATIONS IN WESTERN ARCTIC SNOW AND SEA ICE COVER, 8th Conference on Polar Meteorology and Oceanography, 8.3, The 85th AMS Annual Meeting (San Diego, CA), January 2005

Stone, R.S.; Aerosol and Radiation Monitoring Activities at U.S. and Affiliated Polar Observatories, Tropospheric Aerosol Research at Dome C - ISAC Bologna, Italy 22-23 October 2004.

Stone, R.S., D.C. Douglas, G.I. Belchansky, S.D. Drobot, and J. Harris; Correlated Trends in Western Arctic Snow Cover and Sea Ice Distribution, NOAA Climate Monitoring and Diagnostics Laboratory 2004 Annual Meeting, Boulder, CO, May 24-26, 2004.

Stone, R.S.; Aerosol Monitoring and Diagnostics Activities at U.S. and Affiliated Polar Observatories, POLAR-AOD Network Workshop – ISAC, Bologna, Italy 27-29 October 2003.

Tomasi, C., et al.; Aerosols in Polar Regions, The Second International Conference on Global Warming and the Next Ice Age, and Aerosol Workshop, Santa Fe, N. Mexico, 17- 21 July 2006.

Uttal, T., Xuanji Wang, Robert Stone, Patrick Sheridan, Matthew Shupe, Jeff Key, Studies of Multi-year Variability in Arctic Clouds, SEARCH Open Science Team Meeting, Seattle, Washington, October 27-30, 2003.

References

Fairall, C. W., E. F. Bradley, D. P. Rogers, J. B. Edson, and G. S. Young; Bulk parameterization of air-sea fluxes for Tropical Ocean-Global Atmosphere Coupled-Ocean Atmosphere Response Experiment. *J. Geophys. Res.*, **101**, 3747-3764, 1996.

Levinson, D. H., and A.M. Waple; State of the Climate in 2003, Bulletin of the American Meteorological Society, vol. 85, Issue 6, pp.881-881, 2004; Sections on Diminishing Sea Ice in the Western Arctic Ocean, and Snow melt; Stone et al., 2004.

Persson, P. Ola G., C. W. Fairall, E. L. Andreas, P. S. Guest, and D. K. Perovich; Measurements near the Atmospheric Surface Flux Group tower at SHEBA: Near-surface conditions and surface energy budget. *J. Geophys. Res.* **107**(C10), 8045, doi:10.1029/2000JC000705, 2002.

Schnell et al., eds, NOAA/CMDL Summary Report No. 27 2002-2003: Stone: 1. Polar Aerosol Characterizations; 2. Incursions and Impact of Asian Dust Over Northern Alaska, 3. Western Arctic Meltdown Continues, 2004.

Stohl, A., E Andrews, J. F. Burkhart, C. Forster, D. Kowal, C. Lunder, T. Mefford, J. A. Ogren, S. Sharma, N. Spichtinger, K. Stebel, R. Stone, J. Strom, K. Torseth, and C. Wehrli; Pan-Arctic enhancements of light absorbing aerosol concentrations due to North American boreal forest fires during summer 2004, *J. Geophys. Res*., in press, 2006.

Stone, R. S. (2002), Monitoring aerosol optical depth at Barrow, Alaska and South Pole; Historical overview, recent results, and future goals, Proceedings of the 9th Workshop Italian Research on Antarctic Atmosphere, Rome, Italy, 22-24 October 2001, edited by M. Colacino, pp. 123-144, Ital. Phys. Soc., Bologna, Italy.

Stone, R., G. Anderson, E. Andrews, E. Dutton, J. Harris, E. Shettle, and A. Berk; Asian dust signatures at Barrow: observed and simulated, IEEE Workshop on Remote Sensing of Atmospheric Aerosol, An Honorary Workshop for Prof. John A. Reagan, 5-6 April 2005a, University of Arizona, Tucson Arizona, USA, 74-79, 2005. ftp://ftp.cmdl.noaa.gov/pub/betsy/IEEEStoneetal2005.pdf

Stone, R.S., D. Douglas, G. Belchansky, and S. Drobot; Correlated Declines in Pacific Arctic Snow and Sea Ice Cover, *Arctic Research U.S*., NSF, Arlington, VA, Vol. 19, 18-25, 2005.

Stone, R. S., E.G. Dutton, J.M. Harris, andD. Longenecker, Earlier spring snowmelt in northern Alaska as an indicator of climate change, *J. Geophys. Res*. 107(D10)10.1029/2000JD000286, 2002.